MEASUREMENTS OF GONG LOW-DEGREE P-MODE PARAMETERS

M.C. Rabello-Soares[1], **T. Appourchaux**[2]

[1]Teoretisk Astrofysik Center, Danmarks Grundforskningsfond, and
Institut for Fysik og Astronomi, Aarhus Universitet, DK-8000 Aarhus C, Denmark
[2]Space Science Department of ESA, ESTEC, NL-2200 AG Noordwijk

ABSTRACT

Low-degree solar p modes observed by the GONG network have been analysed for $\ell \leq 6$ yielding accurate measurements of their frequencies, splittings and linewidths. The results obtained show significant improvement over the GONG project parameters especially for minimizing the bias on the splitting and the error bars. We used a new method of fitting helioseismic spectra where, instead of fitting the power spectra, we fitted the Fourier spectra involving the knowledge of the mode leakage matrix. The effect of an imperfect knowledge of the $\ell = 1$ leakage matrix upon the splitting determination is shown both for power spectra and Fourier spectra fitting. In addition, the effect of the leakage between the modes of different degrees, or spatial alias, upon the splitting coefficient is analysed. A procedure for cleaning the spatial alias is described leading to splitting coefficients with smaller systematic errors than before.

Key words: Sun: oscillations; Sun: interior.

1. INTRODUCTION

When the solar image is resolved a very large number of modes can be detected making the data analysis very complicated. In order to extract a single (ℓ, m) mode from resolved observations, spherical harmonic decomposition of each image is estimated. Unfortunately, since only half of the Sun is observed, it is essentially impossible to isolate individual modes based on their angular dependence alone.

Since the modes are not completely isolated, the Fourier transform for a given (ℓ, m) mode (y_i) is not given by a Fourier transform of a single mode (x_i), but rather as a sum over the modes contributing to the given spectrum, which can be expressed as: $y_i(\nu) = \sum_j C_{ij}\ x_j(\nu)$ where C gives the contribution from each mode and is called the leakage matrix. This is a rather important point to be considered in the fitting of the data. Not taking into account the spurious modes on a given (ℓ, m) mode spectrum or even taking them into account in a wrong way will produce erroneous determination of the p-modes parameters, as we have already pointed out: Appourchaux et al. (1995) and Rabello-Soares et al. (1997). Here we will present the preliminary results of a very careful analysis of the low degree solar p modes observed by GONG network with special care put on the treatment of spatial mode leakage.

2. DATA ANALYSIS

A maximum likelihood method was used to fit the peaks in the spectra of observational time series and to measure with accuracy the frequencies, widths and amplitudes of the p-modes. In this work, instead of fitting the p modes in power spectra assuming that their statistical distribution is a χ^2 with 2 degrees of freedom (Woodard 1984) as is usually done, we fitted the p modes in the Fourier spectra assuming that the statistics of the Fourier spectrum is a multi-normal distribution (Schou 1992). The main difference between the two methods is in the way they treat the correlation due to the mode leakage. When fitting the $2\ell + 1$ power spectra for a given (ℓ, n) mode, the leakage is taken into account in the modelling of each m spectrum but still assuming that the $2\ell+1$ spectra are statistically independent from each other. On the other hand, when fitting the $2\ell + 1$ Fourier spectra for a given (ℓ, n) mode, the leakage is also taken into account but assuming now that the $2\ell + 1$ spectra are statistically dependent upon one another. For a detailed discussion on this, see Schou (1992) and our previous works: Appourchaux et al. 1998a and 1998b - hereafter: Paper I and II, respectively.

We have applied this fitting technique to 360 days of GONG data (Harvey et al. 1996) starting from 23 August 1995 to 16 August 1996 with a 87% duty cycle. After a spherical harmonic decomposition, an FFT was applied to the whole time series.

A Lorentzian profile was used as a model of the variance of the spectrum of a single mode (n, ℓ, m). We adjusted a linewidth for the entire multiplet (see Appourchaux et al. 1995 and Rabello-Soares et al. 1997) and the same amplitude and background noise for the $\pm m$ modes. The central frequency is given by:

$$\nu_{n\ell m} = \nu_{n\ell} + \sum_{i=1}^{N} a_i(n,\ell)\mathcal{P}_i^{(\ell)}(m) \qquad (1)$$

where $\nu_{n\ell}$ is the mean frequency of a mode multiplet and $\mathcal{P}_i^{(\ell)}(m)$ are orthogonal polynomials defined by: $\mathcal{P}_i^{(\ell)}(\ell) = \ell$ and $\sum_{m=-\ell}^{\ell} \mathcal{P}_i^{(\ell)}(m)\mathcal{P}_j^{(\ell)}(m) = 0$ for i≠j. The polynomials $\mathcal{P}_i^{(\ell)}(m)$ can be expressed in terms of the Clebsch-Gordan coefficients (Pijpers 1997). For $\ell = 1$, we adjusted only a_1 ($N = 1$); for $\ell = 2$ and 3, only a_1, a_2 and a_3 ($N = 3$); and for $\ell \geq 4$, a_1-a_5 ($N = 5$).

As already mentioned, an important point in the p-mode parameter determination is the correct determination of the leakage matrix C in the fitting of the power spectra as well as the Fourier spectra. The leakage matrix of the GONG data is calculated as described in Paper II, after Schou & Brown (1994). Although the leakage matrix changes throughout the year due to the B_0 angle variation, as we are analysing a one-year time series, we are going to suppose that this variation averages out. We took into account the contribution of the $2\ell + 1$ m's in a given (ℓ, m) spectrum. We have fitted at intervals of 17 μHz for $\ell \leq 2$ and 22 μHz for $\ell \geq 3$ around the frequency of a given (n, ℓ, m) mode. An estimate of the uncertainties on the fitted parameters were obtained from the inverse of the Hessian matrix (see Paper I).

3. COMPARISON BETWEEN THE METHODS

We compared the p-mode parameters found by fitting power spectra with those found by fitting Fourier spectra for $\ell \leq 3$ modes. The same initial parameters and the same leakage matrix were used in both fittings.

Their multiplet mean frequencies coincide within 1σ (using combined errors) and the weighted average over n of their absolute frequency difference is smaller than ~ 0.01 μHz for $\ell \leq 3$.

Figure 1 presents the a_1 splitting coefficients found from fitting the Fourier spectra (circles) and the power spectra (stars) for $\ell = 1$. Although the difference between the coefficients is inside the error bars (except for one mode), it is very important. We are looking at the same data, so this difference is a systematic effect due to the fitting process. We can see clearly that the splittings found fitting the power spectra are much more scattered and their weighted average is overestimated by 16 nHz in relation to the Fourier fitting. Also their error bars are bigger, in particular for high frequency modes where they are 40% higher.

As expected, the difference between the two approaches diminishes for higher degrees. In fact, for $\ell = 2$, the a_1 weighted average over n is overestimated by only 3 nHz fitting the power spectra and, for $\ell = 3$, they agree quite well. However, there is still a significant improvement in the error bars. We can conclude that the Fourier fitting is very important for determining $\ell = 1$ mode parameters and is still important for $\ell = 2$ and 3 modes because it calculates all their parameters with the smallest bias and error bars.

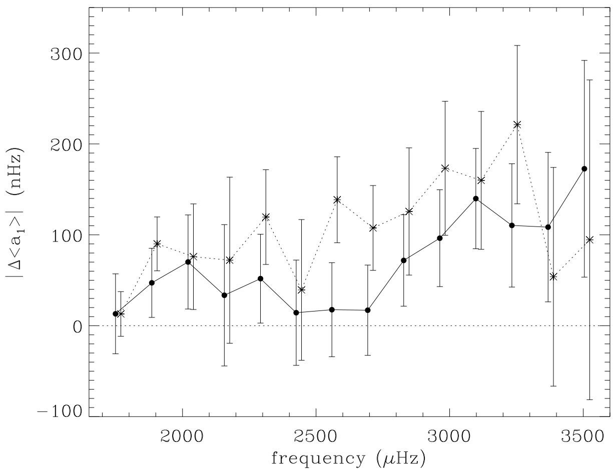

Figure 1. Absolute difference between the a_1 coefficients and their weighted mean over n for $\ell = 1$ fitting the power spectra (stars) and the Fourier spectra (circles). The measurements are slightly displaced in frequency for a better visualization. The weighted average values fitting the power and the Fourier spectra are, respectively: 466 ± 27 nHz and 450 ± 19 nHz (in sidereal units).

4. INFLUENCE OF THE LEAKAGE MATRIX ON THE ROTATIONAL SPLITTINGS DETERMINATION

The correct determination of the leakage matrix is particularly important in the determination of the rotational splittings. A change in the values assumed for the leakage matrix elements will introduce systematic effects on the fitted rotational splittings using Fourier or power spectra. This could be one of the reasons for the discrepancies between the measurements of the splittings by different instruments with spatial resolution.

Due to symmetry properties, for $\ell = 1$, there will be only one matrix element to be determined, i.e. the leakage between $m = -1$ and $m = +1$, which we called α. Using values of α different from that of the theoretical value, α_{th} (section 2), we have determined the rotational splitting a_1 by fitting both the Fourier spectra and the power spectra. The a_1 weighted average over n was calculated using the formal errors computed by the fit (Figure 2).

Figure 2 shows a very interesting result. While a_1 coefficients calculated using the power spectra (stars) vary almost linearly with α, those found using the Fourier spectra (circles) obey a quadratic law. Thus, when fitting the Fourier spectra, the a_1 coefficient could be only underestimated if we use an incorrect value for α, the correct value of α corresponds to the maximum value of the a_1 coefficient. Although these variations in the splitting coefficient are small (around 15 nHz for an error of 20% in α) in comparison to the error bars, they are significant because of their systematic nature.

For ℓ=2, there will be 4 matrix elements to be determined that is the leakage between: m=-2 and 0, m=-2 and +2, m=-1 and +1, m=0 and +2. The a_1 coefficients presents a quadratic variation as for $\ell = 1$

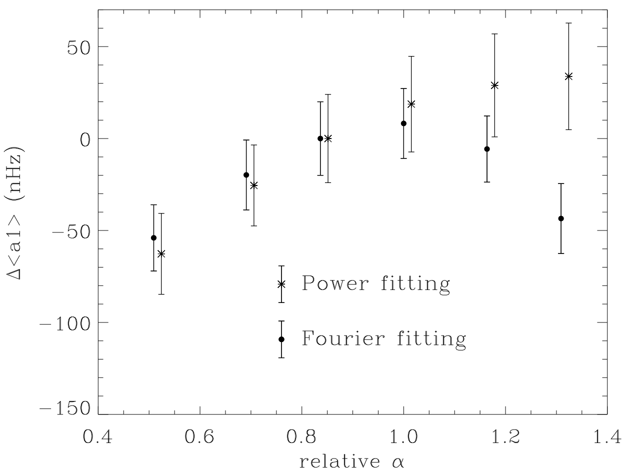

Figure 2. Difference between the weighted average over n of the a_1 coefficients for $\ell = 1$ using a given α and using α_{th}. The x-axis is given relative to a nominal value of $\alpha_{th} = -0.55$.

coefficients when fitting the Fourier spectra. The a_3 coefficient also has a similar behaviour except that the variation in the leakage between m=-1 and +1 shows an inversion in the concavity. The variations of the a_1 coefficients are smaller than 3 nHz for an error of 20% in one of the matrix elements. We limited ourselves in this section to the analysis of $\ell \leq 2$ where the leakage between the modes is more critical because of the small number of elements in the multiplet.

5. LEAKAGE BETWEEN DIFFERENT DEGREES

So far we have mentioned only the leakage between the elements of a given multiplet. However, it is also possible to have leakage between different multiplets, i.e., modes with different degrees. The leakage will be due to modes with a degree similar to the target mode; modes with a very different degree will have a negligible amplitude in the target spectrum. On the other hand, we are going to be concerned by the leakage of modes having a frequency close to that of the target mode, in the range $\sim$ 1500 to 4000 μHz. Figure 3 shows the frequencies of the modes plotted in an echelle diagramme tuned for $\ell = 2$; we can see that the $\ell = 6$ overlap with the $\ell = 1$ modes, $\ell = 7$ overlap with $\ell = 4$ modes and so on.

The influence of the leakage of $\ell = 6$ and 9 modes in the determination of the $\ell = 1$ splitting coefficients can be clearly seen in Figure 1 (circles) as a step for $\nu \geq 2800$ μHz. However, as the mode degree increases, the fitting of the spectra becomes less sensitive to the leakage. In fact, for $\ell = 2$ and 3, there is no clear influence, which is also probably because the overlapping modes have a very different degree than the target. On the other hand, for $\ell \geq 4$, it appears in the GONG data only as a second order effect: a bump in a_2 coefficients (Figure 4). These higher degree modes have much more elements in the multiplet which enable a much better determination

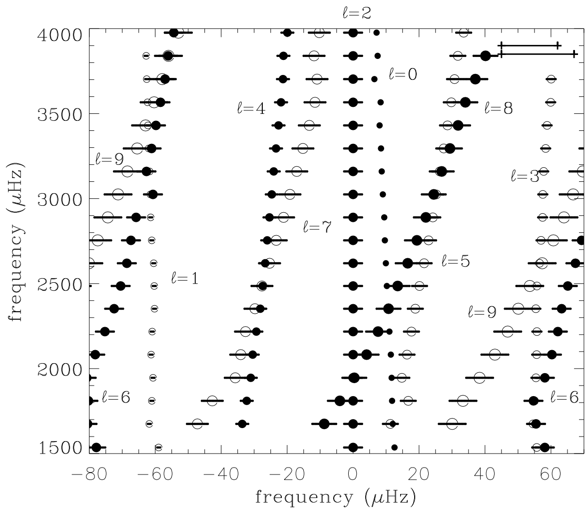

Figure 3. Echelle diagramme centered on $\ell = 2$. The even degree modes are indicated as full circles and the odd modes as empty circles. The size of the circles is proportional to the degree. The horizontal bar crossing the circles represents the splitting due to the solar rotation (2ℓ+1) and is proportional to its size. The horizontal bars on the top right are the window sizes used in the fitting of the modes: for $\ell \leq 2$ (smaller) and for $\ell \geq 3$ (larger).

of the splitting coefficients independently of the influence of the leakage, which is not present in all the 2ℓ+1 observed spectra of the multiplet in the same way.

To correct for the ℓ leakage, the straightforward way is to use a more complete leakage matrix in the likelihood function to be minimized. Unfortunately, this is an extremely computer intensive task because we have to fit more than one multiplet at the same time. Instead, we constructed a more complete leakage matrix and applied its inverse to the observed Fourier spectra as described in Paper I and II, therefore obtaining the 'cleaned' spectra (Figure 4): $\tilde{x} = C^{-1}y$ (see section 1). This method could be used for power spectra fitting as well.

6. RESULTS

Finally, we are going to describe our final results for the fitting of the low degree p-mode parameters using GONG data and compare with others found in the literature. It is well known that using high spatial observations it is very difficult to measure the low degree parameters with a good quality as with integrated light observations making necessary to combine two sets of data: one for low degree data obtained from an integrated light instrument and another for high ℓ using an instrument with high spatial resolution. However, the results presented here are as good as those obtained with integrated light observations. In this way we made possible the creation in the future of a homogeneous set of frequencies and rotational splittings to estimate the solar structure and rotation curve respectively inside the solar interior.

In our final results, we used the 'cleaned' spectra for $\ell = 1$, 4, 5 and 6. For $\ell = 2$ and 3, it is not neces-

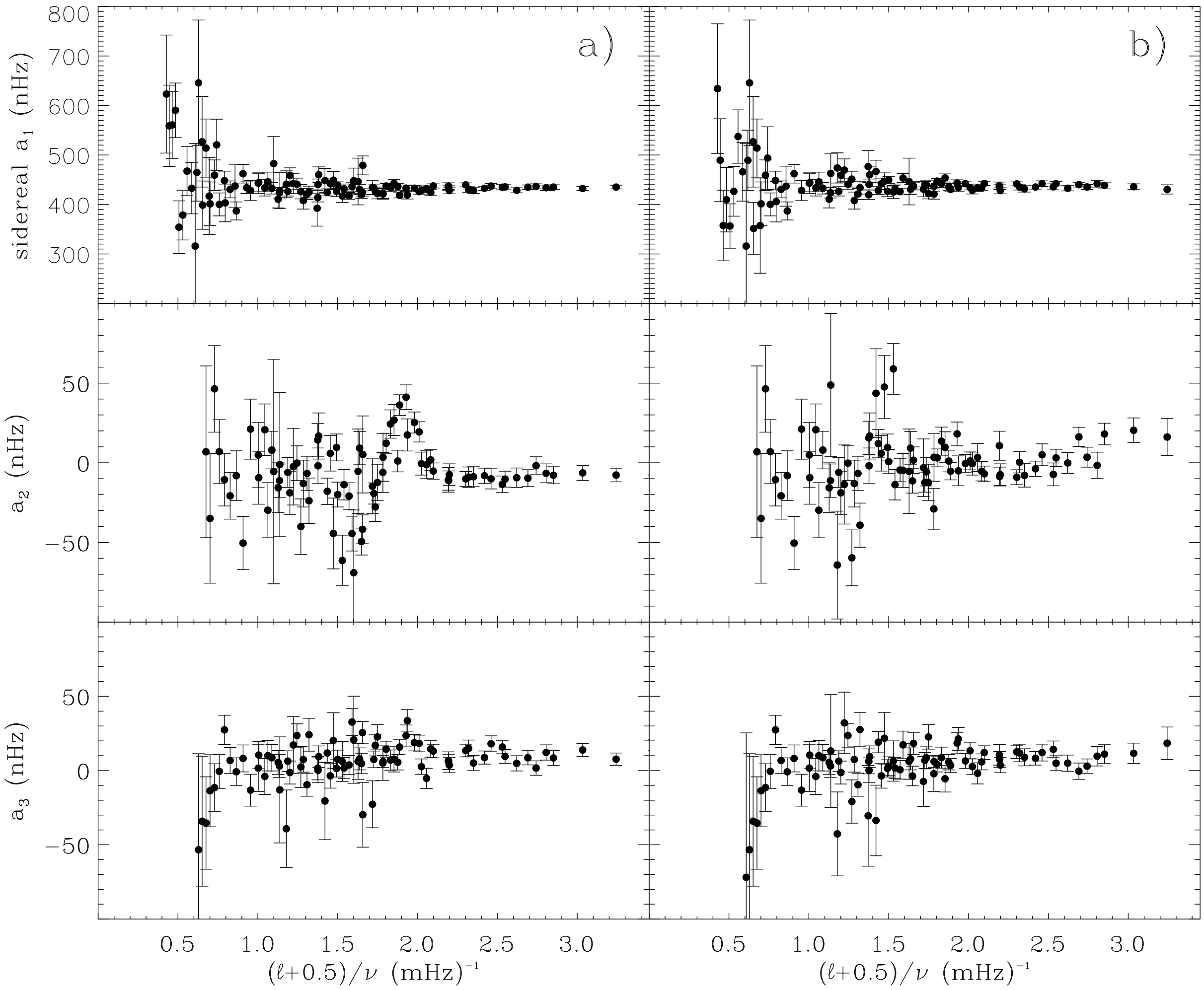

Figure 4. a) Splitting coefficients for the GONG data. Note the step in the a_1 coefficients for $\ell = 1$ and the bump in a_2 coefficients for $\ell = 4$, 5 and 6 modes. b) Splitting coefficients found after 'cleaning' $\ell = 1$, 4, 5 and 6 spectra. Both features in a_1 and a_2 disappeared.

sary to use 'cleaned' spectra because the fit procedure takes care implicitly of the m leaks. We fitted the Fourier spectra instead of the power spectra for all ℓ, except for $\ell = 0$. The variance of the spectrum of a single mode was represented by a Lorentzian profile.

6.1. Frequencies

The final frequency results are shown in Table 1. We have identified 120 p-modes with $\ell \leq 6$ (68 modes with $\ell \leq 3$) with an error smaller than 0.3 μHz.

We have compared our frequencies with those of the GONG project for a time series with the same starting date but twice as short (Hill et al. 1996). Its number of identified modes for $\ell \leq 3$ is very small. There is no systematic difference. We have also compared our frequencies with those of the GOLF/SOHO instrument (Lazrek et al. 1997). They used an 8-month observational period, of which 4 months overlap with the GONG observations used here. Their frequencies are in good agreement with ours.

6.2. Splitting Coefficients

Figure 4b shows the final splitting coefficients found for $\ell = 1$ up to 6 as a function of the turning-point position. The coefficients for $\ell = 1$ and high-order $\ell = 2$ modes are very scattered and have larger error bars than the others. The reason for this bad determination is due to the small number of elements in the multiplet. Comparing with GOLF/SOHO determinations (Lazrek et al. 1997), our error bars are smaller but our measurements are much more scattered for $\ell = 1$ modes. However, for $\ell = 2$ and 3 modes, our data are less scattered and the error bars are much smaller. For a comparison with a low spatial resolution instrument (LOI/SOHO), see Appourchaux et al. 1998c (Figure 6). The weighted averages over n of sidereal a_1 coefficients and their errors (in nHz) are:

	ℓ=1	ℓ=2	ℓ=3	ℓ=4	ℓ=5	ℓ=6
order	11-24	8-28	9-23	9-26	11-26	11-24
	429±17	432±5	431±2	436±2	439±2	440±1

They agree with others measurements found in the literature (see Appourchaux 1998 for a comparison).

6.3. Linewidth

Finally, the mode linewidths are shown in Figure 5. The values found here agree well with the ones measured by GOLF (Lazrek et al. 1997) and VIRGO/SOHO (Fröhlich et al. 1997). The exponential behaviour of the widths is clearly visible for all degrees, except between $\sim$ 2300 and 3100 μHz where a 'plateau' is visible. Note that the dip around 3000 μHz reported by Fröhlich et al. (1997) is fairly visible and it is consistent for all modes with $\ell \leq 6$.

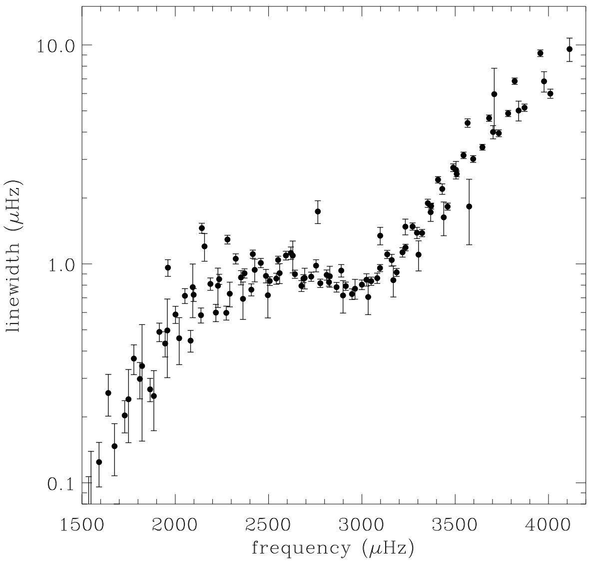

Figure 5. Linewidths of the p-modes.

Table 1. Frequencies and errors in μHz as measured by GONG.

n	ℓ=0	ℓ=1	ℓ=2	ℓ=3
9			1535.86±0.03	1591.54±0.01
10	1548.42±0.04	1612.73±0.01	1674.53±0.01	1729.08±0.01
11	1686.56±0.01	1749.24±0.03	1810.26±0.02	1865.27±0.01
12	1822.08±0.06	1885.07±0.03	1945.73±0.03	2001.18±0.02
13	1957.42±0.07	2020.84±0.05	2082.07±0.02	2137.74±0.02
14	2093.52±0.08	2156.71±0.07	2217.62±0.02	2273.36±0.02
15	2228.64±0.07	2291.95±0.04	2352.16±0.03	2407.58±0.02
16	2362.79±0.06	2425.58±0.05	2485.88±0.03	2541.61±0.02
17	2496.12±0.06	2559.14±0.04	2619.60±0.03	2676.13±0.02
18	2629.54±0.07	2693.33±0.04	2754.38±0.03	2811.37±0.02
19	2764.01±0.07	2828.10±0.04	2889.48±0.03	2946.95±0.02
20	2898.93±0.05	2963.22±0.04	3024.69±0.02	3082.22±0.02
21	3033.71±0.05	3098.15±0.05	3159.85±0.03	3217.65±0.03
22	3168.53±0.06	3232.98±0.05	3294.98±0.03	3353.38±0.03
23	3303.45±0.07	3368.40±0.06	3430.62±0.05	3489.45±0.04
24	3438.66±0.10	3504.15±0.09	3566.48±0.07	
25	3574.83±0.21		3702.93±0.09	
26	3709.39±0.29		3839.84±0.13	
27			3976.24±0.20	
28	3983.36±0.71		4112.74±0.29	

n	ℓ=4	ℓ=5	ℓ=6
9	1640.92±0.02		
10	1778.01±0.02		1864.95±0.00
11	1914.70±0.02	1960.51±0.02	2003.88±0.04
12	2051.63±0.02	2098.42±0.02	2142.36±0.03
13	2188.28±0.02	2235.32±0.02	2279.70±0.02
14	2324.01±0.02	2371.03±0.02	2415.40±0.02
15	2458.45±0.02	2506.02±0.02	2550.99±0.02
16	2592.95±0.02	2641.14±0.02	2687.02±0.02
17	2728.34±0.02	2777.27±0.02	2823.68±0.02
18	2864.13±0.02	2913.65±0.02	
19	3000.04±0.02	3049.86±0.02	3097.19±0.02
20	3135.78±0.02	3186.15±0.02	3233.88±0.02
21	3271.61±0.03	3322.47±0.03	3370.84±0.03
22	3408.01±0.04	3459.25±0.03	3508.08±0.03
23	3544.63±0.04	3596.26±0.05	3645.91±0.04
24	3681.67±0.06	3733.69±0.06	3783.76±0.06
25	3818.72±0.08	3871.61±0.08	3921.86±0.08
26	3956.31±0.11	4009.77±0.12	4060.56±0.11
27	4093.98±0.18		

ACKNOWLEDGMENTS

This work utilizes data obtained by the Global Oscillations Network Group (GONG) project, managed by the National Solar Observatory, a Division of the National Astronomy Observatories, which is operated by AURA, Inc. under cooperative agreement with the National Science Foundation. The data were acquired by instruments operated at Big Bear Solar Observatory, High Altitude Observatory, Learmonth Solar Observatory, Udaipur Solar Observatory, Instituto de Astrofísica de Canarias, and Cerro Tololo Interamerican Observatory.

REFERENCES

Appourchaux, T., 1998, these Proceedings

Appourchaux, T., Toutain, T., et al., 1995, A&A 294, L13

Appourchaux, T., Gizon, L. & Rabello-Soares, M.C., 1998a, A&A (in press)

Appourchaux, T., Rabello-Soares, M.C. & Gizon, L., 1998b, A&A (in press)

Appourchaux, T. and the VIRGO team, 1998c, these Proceedings

Fröhlich, C., Andersen, B.N., et al., 1997, IAU Symposium 181: 'Sounding Solar and Stellar Interiors', eds. J. Provost and F.X. Schmider, Dordrecht, D. Reidel, p. 67

Harvey, J.W., Hill, F., et al., 1996, Science 272, 1284

Hill, F., Stark, P.B., et al., 1996, Science 272, 1292

Lazrek, M., Baudin, F., et al., 1997, Sol. Phys. 175.2, 227

Pijpers, F.P., 1997, A&A 326, 1235

Rabello-Soares, M.C., Roca Cortés, T., et al., 1997, ApJ 480, 840

Schou, J., 1992, PhD Thesis, 'On the Analysis of Helioseismic Data', Aarhus University, Aarhus, Denmark

Schou, J. & Brown, T.M., 1994 A&AS 107, 541

Woodard, M., 1984, PhD Thesis, 'Short-Period Oscillations in the Total Solar Irradiance', University of California, San Diego, Dept. of Physics